OXFORD

Cerebral Cortex, July 2021;31: 3254–3265

doi: 10.1093/cercor/bhab006
Advance Access Publication Date: 24 February 2021
Original Article

ORIGINAL ARTICLE

Accelerated Aging of the Amygdala in Alcohol Use Disorders: Relevance to the Dark Side of Addiction

Dardo Tomasi[1], Corinde E. Wiers[1], Peter Manza[1], Ehsan Shokri-Kojori[1], Yonga Michele-Vera[1], Rui Zhang[1], Danielle Kroll[1], Dana Feldman[1], Katherine McPherson[1], Catherine Biesecker[1], Melanie Schwandt[1], Nancy Diazgranados[1], George F. Koob[2], Gene-Jack Wang[1] and Nora D. Volkow[1]

[1]National Institute on Alcohol Abuse and Alcoholism, Bethesda, MD 20892, USA and [2]National Institute on Drug Abuse, Bethesda, MD 21224, USA

Address correspondence to Dardo Tomasi, 10 Center Dr, Rm B2L124, Bethesda, MD 20892-1013, USA. Email: dardo.tomasi@nih.gov.

Abstract

Here we assessed changes in subcortical volumes in alcohol use disorder (AUD). A simple morphometry-based classifier (MC) was developed to identify subcortical volumes that distinguished 32 healthy controls (HCs) from 33 AUD patients, who were scanned twice, during early and later withdrawal, to assess the effect of abstinence on MC-features (Discovery cohort). We validated the novel classifier in an independent Validation cohort (19 AUD patients and 20 HCs). MC-accuracy reached 80% (Discovery) and 72% (Validation). MC features included the hippocampus, amygdala, cerebellum, putamen, corpus callosum, and brain stem, which were smaller and showed stronger age-related decreases in AUD than HCs, and the ventricles and cerebrospinal fluid, which were larger in AUD and older participants. The volume of the amygdala showed a positive association with anxiety and negative urgency in AUD. Repeated imaging during the third week of detoxification revealed slightly larger subcortical volumes in AUD patients, consistent with partial recovery during abstinence. The steeper age-associated volumetric reductions in stress- and reward-related subcortical regions in AUD are consistent with accelerated aging, whereas the amygdalar associations with negative urgency and anxiety in AUD patients support its involvement in the "dark side of addiction".

Key words: alcoholism, reward, stress, morphometry, age, withdrawal

Introduction

Alcohol use disorders (AUDs) are associated with marked changes in brain structure that have been ascribed in part to alcohol's acceleration of aging, including ventricular enlargement and gray matter (GM) atrophy, particularly in frontal and anterior superior temporal cortices and insula (Pfefferbaum et al. 1998; Thayer et al. 2016; Guggenmos et al. 2017; Sullivan et al. 2018; Zahr et al. 2019; Zhao et al. 2020). There is also evidence of accelerated aging in subcortical regions with AUD including the hippocampus, thalamus, and cerebellum, although to our knowledge accelerated aging of the amygdala has not been reported. However, the brain morphological changes associated with AUD may recover as evidenced by preclinical and clinical studies showing reductions in ventricular enlargement and GM atrophy with alcohol detoxification (Zahr et al. 2016; Zou et al. 2018). Surprisingly, despite the prominence of neurobiological adaptations in the amygdala and other subcortical structures associated with the development of negative emotional states during alcohol withdrawal (Koob and Volkow 2016), mostly derived from preclinical studies (Koob and Le Moal 2005), there are few clinical reports involving

neurobiological studies of negative emotional states in AUD (Ramirez et al. 2020). Further, the effects of detoxification and age on the amygdala and other subcortical regions are less clear.

Machine learning (ML) is being utilized to classify AUD vs. healthy control (HC) groups and identify features that distinguish them. For instance, a support vector machine (SVM) classifier that distinguished AUD participants from non-dependent controls with high accuracy identified cortical thickness in limbic, parietal, and frontal areas and the volumes of the amygdala and the hippocampus as prominent features (Mackey et al. 2019). Thus, we hypothesized that, based solely on subcortical volumes, ML methods would classify AUD patients and HCs with high accuracy, and that the amygdala would emerge as one prominent feature of the classifier. We aimed to study the effects of alcohol, age, and alcohol detoxification on the subcortical features that emerged from the ML classifier, as well as the association between these features and the clinical characteristics of AUD patients.

Thus, we developed a morphometry-based classifier (MC), a simple ML method based on the popular connectome-based predictive modeling (Shen et al. 2017), to classify 33 AUD patients and 32 matched HCs based on subcortical volumes obtained from high-resolution 3 T magnetic resonance imaging (MRI). To assess brain recovery with detoxification, AUD patients were scanned twice, 2 weeks apart, during early and late inpatient detoxification. We hypothesized that with subcortical volumes MC would achieve higher classification accuracy than with cortical morphometrics, that its performance would be similar to that of SVM (H1) and that the amygdala would emerge as a prominent MC-feature (H2). We also tested the generalizability of our MC-model in an independent AUD and HC validation cohort (H3). Consistent with the age×alcohol interaction effects on brain structures, we hypothesized that the subcortical regions identified by MC, including the amygdala, would show accelerated aging in AUD (H4), that the volume of the amygdala would recover during detoxification (H5), and it would be associated with negative emotions (impulsivity, anxiety, compulsivity, and negative emotionality [NEM]) while controlling for age and detoxification (H6).

Materials and Methods

Discovery cohort

Thirty-three AUD patients and 32 HCs participated in the study. The two groups did not differ in age or gender proportion (Table 1). All subjects were screened to exclude ferromagnetic implants which are contraindicated for MRI, major medical, neurological and psychiatric disorders, head trauma, chronic use of psychoactive medications, current or past diagnosis of substance use disorder (other than alcohol abuse and/or dependence in the AUD group, or current tobacco smoking in either group) as assessed by the Structured Clinical Interview for the *Diagnostic and Statistical Manual of Mental Disorders* (*DSM-IV*; American Psychiatric Association 2000) or *DSM-5* (American Psychiatric Association 2013). Women were neither pregnant nor breastfeeding. AUD participants were admitted for detoxification and had at least 5 years' history of heavy drinking. Alcohol was the preferred drug for all AUD patients. They completed 3 weeks detoxification in the inpatient unit of the National Institute of Alcohol Abuse and Alcoholism. All participants had a negative breath test result for alcohol consumption and a negative urine drug screen on days of testing (except for benzodiazepines in AUD patients) and were free of psychoactive medications within 24 hours of study procedures (except benzodiazepines during early detoxification for AUD patients). All subjects provided written informed consent to participate in the study, which was approved by the Institutional Review Board at the National Institutes of Health (Combined Neurosciences White Panel).

Alcohol withdrawal and benzodiazepine use

In the NIAAA detoxification clinic, AUD patients were assessed with the Clinical Institute Withdrawal Assessment-Alcohol revised (CIWA-Ar) (Sullivan et al. 1989) at admission and then approximately every 2 hours until withdrawal ceased. If the CIWA-Ar scores were >8, patients were given benzodiazepines to treat withdrawal symptoms, which 26 patients received (23 oxazepam, 3 diazepam).

Ratings and neuropsychological testing

One week after admission (baseline), participants completed the Alcohol Use Disorders Identification Test (AUDIT) as a measure of harmful alcohol consumption (Saunders et al. 1993), the Timeline Followback (TLFB) to assess daily alcohol consumption in the 90 days prior to the study (Sobell and Sobell 1996), the Lifetime Drinking History (LDH) to assess lifetime alcohol consumption (Skinner and Sheu 1982), and the Alcohol Dependence Scale (ADS) to assess the severity of dependence (Skinner and Allen 1982). The Fagerström test was used as a measure of nicotine dependence and the Wechsler Abbreviated Scale of Intelligence (WASI-II) subtests Matrix Reasoning and Vocabulary as a proxy for general intelligence (Wechsler 1999). Participants also completed the State–Trait Anxiety Inventory (STAI) (Spielberger et al. 1983), the Obsessive-Compulsive Drinking Scale (OCDS) to assess obsessive and compulsive alcohol thinking and drinking behaviors (Anton et al. 1996), and the Beck Depression Inventory (BDI) to assess depression symptoms (Beck et al. 1988). The multidimensional personality questionnaire (MPQ) was used to rate trait measures of NEM (Tellegen and Waller 2008). The UPPS-P Impulsive Behavior Scale was used to assess negative urgency (Cyders et al. 2007).

MRI acquisition

At baseline (within one week of last alcohol use) participants in the Discovery cohort underwent MRI on a 3.0 T Magnetom Prisma scanner (Siemens Medical Solutions USA, Inc., Malvern, PA) equipped with a 32-channel head coil. T1-weighted 3D magnetization-prepared gradient-echo (MP-RAGE, TR/TE = 2400/2.24 ms) and variable flip angle turbo spin-echo (TR/TE = 3200/564 ms) pulse sequences were then used to acquire high-resolution anatomical brain images with 0.8 mm isotropic voxels, field-of-view (FOV) = 240 × 256 mm, matrix = 300 × 320, and 208 sagittal slices.

To validate our classifier with different data acquisition procedures and conditions, AUD patients in the Discovery cohort underwent two additional structural scans, one collected at baseline (week 1) and the other at the end of the 3-weeks detoxification period (week 3), using a "low-resolution" MRI protocol including MP-RAGE (TR/TE = 2200/4.25 ms; FA = 9°, 1-mm isotropic resolution) and T2-weighted multi-slice spin-echo (TR/TE = 8000/72 ms; 1.1-mm in-plane resolution; 94 slices, 1.7-mm slice thickness) pulse sequences. This data was used to assess the effect of alcohol withdrawal on subcortical volumes.

Table 1 Characteristics of AUD patients and HCs in the Discovery and Validation cohorts

	AUD ($n=33$)	HC ($n=32$)	P-value	AUD ($n=19$)	HC ($n=21$)	P-value
		Discovery			Validation	
Demographics						
Age [years]	40.5 ± 12.9	42.4 ± 12.1	NS	47.6 ± 10.1	46.8 ± 10.5	NS
Gender [males/females]	23/10	20/12	NS*	14/5	13/8	NS*
Education [years]	13.2 ± 2.7	15.7 ± 1.7	1E-04	12.4 ± 2.9	15.2 ± 2.4	0.002
BMI [kg/m^2]	26 ± 5	26 ± 6	NS	27 ± 5	29 ± 6	NS
Number of smokers/no smokers	19/14	0/32	<1E-06*	10/9	0/21	<1E-04*
Premorbid cognition and psychiatric symptoms						
Intelligence quotient	98 ± 18	116 ± 15	2E-04	90 ± 16	103 ± 16	0.02
Anxiety score	52.0 ± 11.2	29 ± 8	2E-17	39 ± 12	29 ± 8	1E-03
OCDS obsessive score	8.8 ± 4.9	0.1 ± 0.2	5E-15	4.4 ± 4.1	0.2 ± 0.7	2E-04
OCDS compulsive score	13.5 ± 3.5	1.0 ± 1.1	4E-28	7.7 ± 5.1	0.7 ± 1.3	1E-05
Depression score	19.9 ± 10.5	1.1 ± 0.5	1E-16	7.8 ± 9.9	1.3 ± 1.6	0.01
Urgency score	2.8 ± 0.7	1.5 ± 0.5	7E-14	2.1 ± 0.6	1.5 ± 0.4	0.001
NEM score	44 ± 19	21 ± 12	6E-07	31 ± 16	22 ± 9	0.02
Alcohol use						
TLFB [average drinks per day]	13.8 ± 9.0	0.2 ± 0.25	3E-12	10.6 ± 6.5	0.8 ± 1.0	4E-06
CIWA score	6.0 ± 4.6	0.06 ± 0.35	8E-10	2.2 ± 3.2	0.2 ± 0.6	0.03
AUDIT total score	10.9 ± 1.7	1.6 ± 1.2	2E-34	21.6 ± 8.4	1.6 ± 1.7	3E-09
Alcohol dependence score	22 ± 9	0.3 ± 0.6	4E-21	13 ± 7	0.2 ± 0.4	1E-08
Years of alcohol use	25 ± 13	25 ± 12	NS	30 ± 11	26 ± 14	NS
Number of drinking days/month	26 ± 6	3.8 ± 5.6	4E-22	25 ± 7	2.0 ± 3.0	2E-12
Number of drinks/drinking day	16 ± 9.	1.5 ± 0.6	3E-10	12 ± 9	2.0 ± 1.0	1E-04
Brain volumetry						
ICV [mL]	1296 ± 200	1262 ± 213	NS	1252 ± 231	1283 ± 228	NS
Brain volume [mL]	1111 ± 90	1175 ± 101	4E-04	1085 ± 137	1133 ± 121	NS
Cortical GM [mL]	455 ± 46	486 ± 47	3E-05	431 ± 61	463 ± 52	NS
Cortical WM [mL]	426 ± 49	450 ± 50	5E-03	444 ± 64	460 ± 59	NS
Subcortical GM [mL]	57.1 ± 6.3	62.3 ± 6.2	2E-04	55.1 ± 6.4	56.5 ± 4.2	NS
Ventricles [% of ICV]	27.0 ± 11.1	17.1 ± 6.2	2E-04	23.5 ± 11.1	21.2 ± 11.6	NS
CSF [mL]	1.43 ± 0.31	1.09 ± 0.16	4E-06	1.31 ± 0.29	1.16 ± 0.22	NS
Cerebellar cortex [mL]	113 ± 14	117 ± 11	0.05	102 ± 13	103 ± 10	NS
Cerebellar WM [mL]	27.8 ± 4.1	28.0 ± 3.9	NS	25.3 ± 3.6	26.4 ± 2.8	NS
Corpus callosum [mL]	2.7 ± 0.6	3.0 ± 0.5	0.04	2.6 ± 0.5	2.8 ± 0.4	NS

Note: Two sample *t*-test; *Chi-square test. AUDIT: Alcohol Use Disorders Identification Test; TLFB: Timeline Followback; CIWA: Clinical Institute Withdrawal Assessment-Alcohol revised; OCDS: Obsessive–Compulsive Drinking Scale. The MPQ was used to rate trait measures of NEM. The UPPS-P Impulsive Behavior Scale was used to assess negative urgency (see Supplementary Information).

One AUD patient did not complete the last session due to scheduling problems and was removed from this analysis.

Validation cohort

An independent dataset, consisting of 21 HC and 19 individuals with AUD who were also scanned with the low-resolution MRI protocol during the first week of inpatient detoxification (4 ± 2 days since last alcohol use) (Tomasi et al. 2019), was used to validate the classification results (Table 1). The two groups did not differ in age, gender proportion, or body mass index (BMI). Participants were screened to exclude major medical, neurological and psychiatric disorders, head trauma (with loss of consciousness longer than 30 minutes), chronic use of psychoactive medications, current or past diagnosis of substance use disorder (other than alcohol abuse and/or dependence in the AUD group, or current tobacco smoking in either group) as assessed by the Structured Clinical Interview for the Diagnostic and Statistical Manual of Mental Disorders (DSM-IV), and metallic implants which are contraindicated for MRI. Women were neither pregnant nor breastfeeding and were studied in the mid-follicular phase (3–10 days after the first day of their last period). AUD participants had at least 5 years' history of heavy drinking and were abstinent from alcohol 3.8 days at the time of the scans (range 0–7 days). All participants had a negative urine drug screen on the days of testing and were free of psychoactive medications within 24 hours of study procedures. All participants provided written informed consent to participate, which was in accordance with the Declaration of Helsinki and approved by the Institutional Review Board at the National Institutes of Health (Combined Neurosciences White Panel).

On the day of screening (first study day), participants completed the AUDIT, TLFB, LDH, total lifetime alcohol (TLA), ADS, WASI-II, STAI, OCDS, BDI, and the CIWA. The AUD participants remained in the NIH's clinical center overnight to ensure that they did not ingest any alcohol and were scanned on the following study day. The MPQ was used to rate NEM and the UPPS-P was used to assess negative urgency.

Brain morphometry

T1- and T2-weighted images were carefully reviewed by a radiologist to assess the clinical significance of incidental findings. The structural preprocessing pipelines (Glasser et al. 2013)

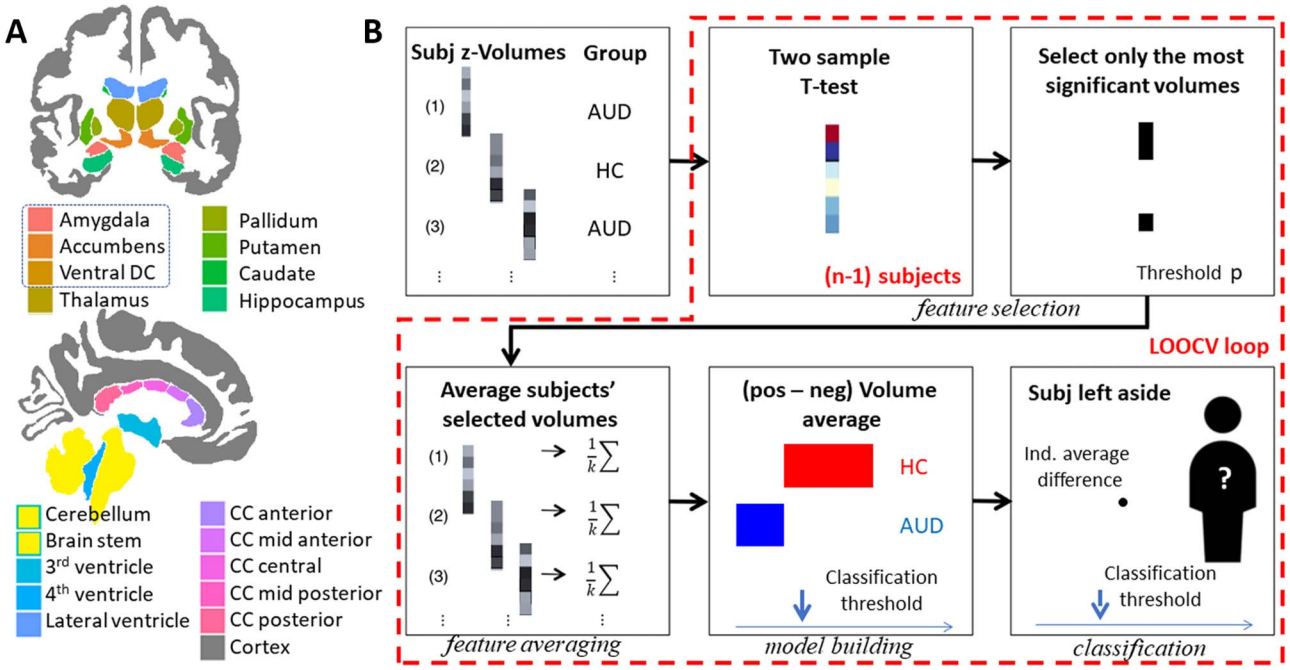

Figure 1. Morphometry-based classification modeling (MC). (A) Coronal (top) and sagittal (bottom) views of a human brain atlas showing 27 (9 bilateral and 9 medial) out of the 45 subcortical volumes assessed with FreeSurfer. These regions-of-interest are relevant in AUD and have been implicated in alcohol craving (hippocampus), intoxication (basal ganglia), and withdrawal (extended amygdala; dashed rounded rectangle), or have been implicated in alcohol-related accelerated aging (lateral ventricles). (B) Standardized subcortical volumes (z-Volumes) and group membership for each of n subjects are the inputs to MC. At each of n iterations, the model is developed using data from n-1 subjects (training set) using leave-one-out cross-validation (LOOCV; dashed red line). Next, a two-sample *t*-test is used to assess group differences in each z-Volume, across all subjects in the training set. Next, the most important z-Volumes are selected as features for further analysis. Next, for each subject, the most important z-Volumes are then averaged, separately for positive (pos: HC > AUD) and negative (neg: AUD > HC) features and the difference between positive and negative averages is calculated for each subject (Zi). Next, a classification threshold is computed by averaging Z-values across all subjects in the training set and the classification threshold is compared with the individual Z-value of the test subject to classify him/her into either AUD or HC. DC: diencephalon; CC: corpus callosum; k: number of features.

of the Human Connectome Project based on FreeSurfer 5.3.0 were used to align the T1- and T2-weighted images, perform bias field correction, register the subject's native structural volume space to the stereotactic space of the Montreal Neurological Institute (MNI), segment the brain into predefined structures, reconstruct white and pial cortical surfaces, and perform FreeSurfer's standard folding-based surface registration. Subcortical segmentation results were inspected for any notable issues (see Supplementary Fig. S1). Forty-five subcortical volumes, defined in the automatic subcortical segmentation atlas (Fischl et al. 2002) were estimated: lateral and inferior-lateral ventricles, cerebellar white matter (WM) and cortex, thalamus, caudate, putamen, pallidum, hippocampus, amygdala, accumbens, ventral diencephalon (DC), WM and non-WM hypointensities, choroid plexus and vessels on each hemisphere and the third, fourth and fifth ventricles, brain stem, cerebrospinal fluid (CSF), optic chiasm, and five partitions of the corpus callosum (CC; anterior, middle anterior, central, middle posterior, and posterior; Fig. 1A).

Machine learning

Confounding effects from differences in intracranial volume, age, and gender were regressed out across subjects, independently for each ROI, before classification in IDL (ITT Visual Information Solutions, Boulder, CO). Here we propose *morphometry-based classification* (MC), a data-driven approach for the prediction of group membership from brain morphometrics. MC relies on leave-one-out cross-validation (LOOCV) for the generalization to independent data and was inspired by connectome-based predictive modeling (CPM) (Shen et al. 2017; Tomasi and Volkow 2020).

At each of *n* iterations, one of the *n* individuals was excluded and the four MC-steps: *feature selection*, *feature averaging*, *model building*, and *classification* were carried across the remaining *n* - 1 individuals to train the model as follows. *Feature selection*: Two-sample *t*-test was used to assess differences in volume, cortical area, thickness, or curvature index between AUD and HC. ROIs with significant group differences were identified as either positive (AUD > HC) or negative (HC > AUD) features and included in the model. Four thresholds were tested ($P < 0.001$, 0.005, 0.01, 0.05) for feature selection to certify that results did not depend on arbitrary threshold selection. *Feature averaging*: ROIs were averaged, independently for positive and negative features, to compute mean positive, X_{n-1}, and negative, Y_{n-1}, averages across ROIs and *n*-1 subjects. Prior averaging, each ROI volume was z-standardized across all subjects to control for differences in volume across ROIs (Fig. 1B) to avoid bias against small ROIs. *Model building*: Since volume increases in some ROIs are frequently accompanied by decreases in other ROIs, the average difference score, $Z_{n-1} = X_{n-1} — Y_{n-1}$, was calculated. *Classification*: Z_{n-1} was then used as a threshold to predict the group membership of the remaining individual from his/her X_1 and Y_1 values (AUD, if $Z_1 > Z_{n-1}$; HC, otherwise). MC-features that overlapped across all LOOCV-iterations were identified. Permutation testing was used to assess the empirical null statistic distribution of

MC results (Shen et al. 2017). Specifically, 1000 MC estimations were carried by randomly reassigning group membership labels, while preserving the structure of the morphometric data. The P-value of the permutation test was computed as the proportion of MC permutations with greater or equal balanced accuracy than the true balanced accuracy of the classifier (Shen et al. 2017). We used balanced accuracy (MC-accuracy, the average of the proportion corrects of each group individually) (Brodersen et al. 2010) instead of regular classification accuracy (the proportion corrects for the whole sample) to account for the imbalance in the number of subjects between groups.

MC was implemented in IDL. MC-accuracy (% correct classification), specificity (true negative rate), and sensitivity (true positive rate) were contrasted against those resulting from the same data using an SVM classifier implemented in R (package e1071 v1.7–3).

Statistical analyses

Statistical testing was carried out in R. Analysis of covariance (ANCOVA: Volume ~ grp*age) with main effects of group and age and age-by-group interactions was used to assess if subcortical volumes predicting group membership are prone to accelerated aging in AUD. A false discovery rate (FDR) corrected pFDR < 0.05 was used to report significant effects of group and age on subcortical volumes. Age-by-group interaction effects on subcortical volumes are reported at $P < 0.05$, uncorrected.

ANCOVA was also used to assess the effects of negative emotions and history of alcohol use on subcortical volumes in AUD. Specifically, we tested for the main effects of impulsivity, obsessive–compulsive drinking, anxiety, NEM, and TLA consumption on subcortical volumes in the AUD group while using the number of heavy drinking years (HDY) and age as covariates (volume ~ urgency + OCDS_total_score + anxiety + NEM + TLA + HDY + age). Significant main effects of negative affect and history of drug use on subcortical volumes are reported at pFDR < 0.05.

A mixed model contrasting subcortical volumes at baseline and the end of detoxification was used to assess the effect of withdrawal on MC-features that distinguished AUD from HC.

Results

Demographic, alcohol use variables, and brain volumetry

Discovery Cohort:

Nineteen AUD patients and none of the HCs were current tobacco smokers ($\chi^2 > 25$, $P < 1E\text{-}06$; Table 1). On average, AUD participants consumed 179 g alcohol per day during the last 90 days. Conversely, 8 of the HC subjects had no alcohol intake during the last 90 days, and the remainder consumed an average of 3 g alcohol per day.

On the first study day, AUD participants had severe withdrawal symptoms (average CIWA score of 6). The AUDIT score was <4 for all HCs and >6 for all AUD participants (Table 1). AUD participants had lower intelligence quotient (IQ) scores and fewer years of education than HC. Impulsivity (urgency score), NEM score, depression (BDI score) and anxiety (STAI score), alcohol craving (obsessive and compulsive OCDS scores), and withdrawal (CIWA score) ratings were higher for AUD than for HC (Table 1).

The estimated volumes of WM and GM and CC were smaller and those of ventricles and CSF were larger for AUD than for HC (Table 1). The cerebellar cortex was smaller for AUD but the cerebellar WM and the intracranial volumes did not differ between AUD and HC. To assess the effect of scan resolution on FreeSurfer estimations we assessed the correlation between volumetric measures obtained from high- and low-resolution scans at baseline, across 45 subcortical volumes and 33 AUD patients, which corresponded to R = 0.998 (Fig. 2A).

Validation Cohort:

Ten of the AUD and none of the HC were smokers ($\chi^2 = 13.9$, $P < 0.0001$). AUD patients drank an average of 136 g alcohol per day in the last 90 days. HC drank 27 g alcohol per day. AUD patients had lower IQ scores than HC ($t = 2.3$, $P = 0.03$) and fewer years of education ($P < 0.001$). Impulsivity, NEM, depression and anxiety, alcohol craving, and withdrawal ratings were higher for AUD than for HC (Table 1). There were no significant differences in brain volumetry between AUD and HC in the Validation cohort.

Morphometry-based classification

Twenty-six MC-features (17 positive and 9 negative features) out of 45 subcortical volumes distinguished AUD from HC at baseline, using a feature selection threshold $P < 0.01$ in the Discovery cohort. The third ventricle, CSF, WM- and non-WM hypointensities, left-inferior-lateral ventricle, as well as left and right lateral ventricles and choroid plexus, had larger volumes in AUD than HC.

Conversely, the middle posterior, central and middle anterior partitions of the CC, brain stem, left-cerebellar cortex, as well as bilateral amygdala, hippocampus, thalamus, putamen, accumbens, and ventral DC (hypothalamus, basal forebrain, and sublenticular extended amygdala, and a large portion of ventral tegmentum) had larger volumes in HC than in AUD ($P < 0.02$, two-tailed t-test; Table 2 and Fig. 2B). No additional features emerged at the lowest feature selection threshold ($P < 0.05$). With these features, MC-accuracy reached 80% in the classification of AUD and HC (Fig. 2B). MC-accuracy did not vary significantly as a function of threshold (P-threshold = 0.05, 0.01, 0.005, and 0.001; 75% < MC-accuracy < 80%; $0.012 < P < 0.001$, permutation testing). Using subcortical volumes the MC classifier achieved 86% sensitivity and 76% specificity in this sample. Similar MC-features emerged from AUD's low-resolution images collected at baseline (week 1), and MC- accuracy reached 84% ($P < 0.001$, permutation testing; Fig. 2C). With other morphometrics (cortical volumes, surface areas, cortical thickness, curvature, and/or folding index, using the Destrieux (Supplementary Table S1) or Desikan (not shown) atlases) MC-accuracy, sensitivity and specificity were lower compared to those obtained with the subcortical volumes. For subcortical volumes, balanced accuracy, specificity, and sensitivity were higher for MC than for SVM. With cortical features, the specificity was higher for SVM than for MC (Table S2; $P < 5E\text{-}8$, paired t-test); however, balanced accuracy and sensitivity did not differ significantly between MC and SVM. In the validation cohort (19 AUD and 21 HC), MC-accuracy was 72% ($P < 0.001$, permutation testing), using a feature selection threshold $P < 0.05$ (Fig. 2D). The MC-features for the Validation cohort were larger third ventricle and smaller right-thalamus and left-ventral DC for AUD than HC, whereas using only subcortical volumes SVM-accuracy was 52.5%. The difference in MC-accuracy between the Discovery and Validation

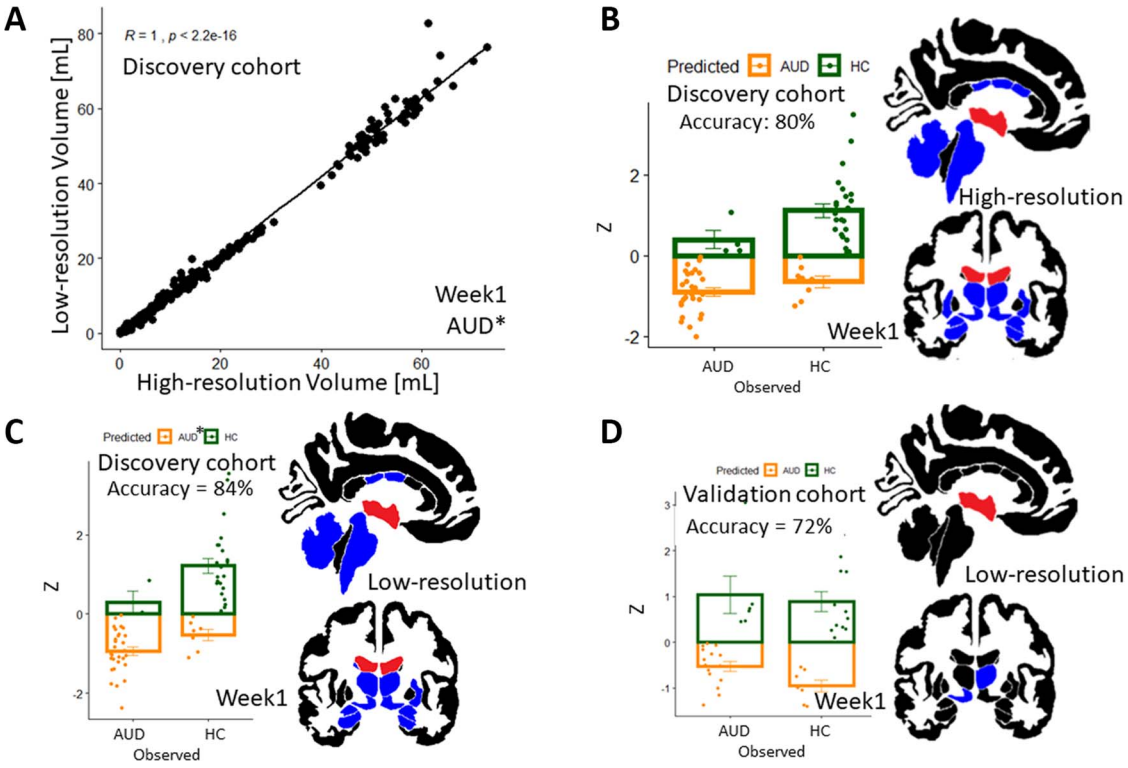

Figure 2. MC classification features and accuracy. (*A*) The volumes of the 45 subcortical regions computed with FreeSurfer from high- and low-resolution T1-weighted images obtained at baseline (week 1) were highly correlated across regions-of-interest and AUD patients ($n = 33$). (*B*,*C*) Bar plot showing that the MC achieved >80% balanced accuracy in the prediction of AUD patients and HCs from 26 subcortical volume features from high (*B*) or low (*C*) resolution data from the Discovery cohort. (*D*) Bar plot showing that MC-accuracy achieved 72% in the prediction of 19 AUD and 21 HC from the Validation cohort using 3 subcortical volume features: the third ventricle (red) consistently showed larger volumes for AUD than for HC; the right thalamus, and left ventral DC (blue) showed larger volumes for HC than for AUD.The coronal (top) and sagittal (bottom) views of a human brain atlas show the features of this classifier for illustrative purposes. The ventricles (red) consistently showed larger volumes for AUD than for HC; the amygdala, hippocampus, basal ganglia (excluding globus pallidus), thalamus, cerebellum, brain stem and medial regions of the corpus callosum (blue) showed larger volumes for HC than for AUD. Z: positive–negative difference score (see text).

cohorts was not significant ($\chi^2 = 2.1$, $P = 0.15$). In addition, the MC model was cross validated by using the MC model and the subcortical volume features for the Discovery cohort to predict group membership in the Validation cohort, using a feature selection threshold $P < 0.01$. With these constraints MC reached a balanced accuracy of 67% in the classification of participants in the Validation cohort.

Effect of age

We first tested the homoscedasticity of the morphometrics using two homogeneity of variance tests, the parametric Bartlett's test (Bartlett 1937), and the non-parametric Fligner-Killeen test (Conover et al. 1981) in the Discovery sample, which revealed minimal differences in the variance of subcortical GM volumes between HC and AUD, but larger differences in the variance of CSF partitions, and confirmed the normal distributions of amygdala volume and its regression slopes for age using the Shapiro–Wilk normality test (Shapiro and Wilk 1965) (Table S3). Then, ANCOVA with an FDR-correction was used to investigate the effect of age on GM features. Eight subcortical GM volumes that differentiated AUD and HC demonstrated significant main effect of age (pFDR < 0.05; Fig. 3). Only the left-amygdala demonstrated age×group interaction effects ($P = 0.04$, uncorrected; Table 2 and Fig. 3*D*), which was confirmed using non-parametric ANCOVA (Young and Bowman 1995) ($P = 0.01$).

Negative emotions and history of alcohol use

The left- and right-amygdala volumes had significant positive associations with both negative urgency and anxiety ($P < 0.05$; Fig. 4 and Table 2) and showed significant interactions between group membership and negative urgency and anxiety ($P = 0.003$). In exploratory fashion, we investigated potential associations between other MC-features and negative emotions using ANCOVA. Only the right-putamen showed significant association with NEM (pFDR < 0.05; Table 2) and NEM × group interaction effects ($P = 0.008$; Fig. 4). The association between left-hippocampus volume and compulsive drinking did not survive FDR-corrections for multiple comparisons. The GM volume in right putamen and accumbens, left-cerebellar cortex and the bilateral thalamus, decreased with TLA ($P < 0.05$; Table 2 and Fig. 4). However, these associations did not survive FDR-corrections for multiple comparisons.

Alcohol Detoxification

We found partial normalization of abnormalities in MC-features with detoxification. Specifically, the third ventricle (6.4%), left-inferior-lateral (24.7%), and bilateral lateral ventricles (4.8%), showed smaller volumes, and the right amygdala (2.7%) and hippocampus (1.4%), left thalamus (1.8%) and cerebellar cortex (0.9%) showed larger volumes at the end of detoxification (week 3) compared to baseline (week 1; pFDR < 0.05; Fig. 5A). The

Table 2 Statistical significance for main effects of group, age, age∗group on subcortical volume features that emerged from morphometric classification of AUD patients and HCs, as well as effects of urgency, obsessive–compulsive drinking (OCDS total score), anxiety (STAI score), NEM score, and TLA on subcortical volume in AUD patients

Volumes	HC ≠ AUD	Age	Age*grp	Urgency	OCDS total	STAI	NEM	TLA
				P-value				
Third ventricle	0.006*	0.0003*	ns	ns	ns	ns	0.05	ns
Brain stem	0.003*	0.2	ns	ns	ns	ns	ns	ns
CC_Central	0.001*	0.01*	ns	ns	ns	ns	ns	0.02
CC_Mid_Anterior	0.02*	0.009*	ns	ns	ns	ns	0.04	ns
CC_Mid_Posterior	0.03*	0.006*	ns	ns	ns	ns	0.05	0.02
CSF	0.00001*	0.03*	ns	ns	ns	ns	0.04	0.04
Left accumbens	0.00004*	0.0002*	ns	ns	ns	ns	ns	ns
Left amygdala	0.003*	0.2	0.04	0.0006*	ns	0.05	ns	ns
Left cerebellar cortex	0.03*	0.0008*	ns	0.06	ns	ns	ns	0.03
Left choroid plexus	0.02*	0.005*	ns	ns	ns	ns	0.004	ns
Left hippocampus	0.00006*	0.04	ns	ns	0.005	ns	ns	ns
Left-inf-lateral ventricle	0.006*	0.1	ns	ns	ns	ns	ns	ns
Left lateral ventricle	0.00004*	0.00004*	ns	ns	ns	ns	0.01	ns
Left putamen	0.007*	0.000004*	ns	0.03	ns	ns	ns	ns
Left thalamus	0.009*	0.09	ns	0.007	ns	0.01	ns	0.01
Left ventral DC	0.0002*	0.0002*	ns	ns	ns	ns	ns	ns
non-WM hypointensities	0.007*	0.0006*	0.009	ns	0.03	ns	ns	ns
Right accumbens	0.004*	0.002*	ns	ns	ns	ns	ns	0.01
Right amygdala	0.006*	0.2	ns	0.01	ns	0.002	ns	ns
Right choroid plexus	0.002*	0.004*	ns	ns	ns	ns	0.04	0.06
Right hippocampus	0.003*	0.1	ns	ns	ns	ns	ns	ns
Right lateral ventricle	0.0001*	0.0000005*	ns	ns	ns	ns	0.009	ns
Right putamen	0.001*	9E-10*	ns	0.06	ns	ns	0.0004*	0.04
Right thalamus	0.0005*	0.1	ns	0.05	ns	0.004	ns	0.05
Right ventral DC	0.0003*	0.000003*	ns	ns	ns	ns	ns	ns
WM hypointensities	0.0006*	0.0007*	ns	ns	ns	ns	ns	ns

Note: *pFDR < 0.05. Statistical model: ANCOVA. Discovery cohort.

recovery of left-amygdala volume (2.1%) did not reach significance. The effect of age on abstinence-related volume recovery was significant only for the right-hippocampus, which showed stronger recovery in younger than in older AUD patients during detoxification (R = -0.33; $P = 0.03$, uncorrected). The abstinence-related volume recovery in right-amygdala was predicted by negative urgency (R = 0.41, $P = 0.04$, two-tailed), and at trend-level by anxiety (R = 0.32, $P = 0.08$, two-tailed) and baseline measures of right-amygdala volume (R = 0.34; $P = 0.06$, two-tailed), suggesting a higher recovery rate for the amygdala volume in individuals with higher negative urgency or anxiety and with larger amygdalae at baseline.

Despite the recovery, at the end of detoxification subcortical volumes were significantly different for AUD patients compared to HC (Fig. 5B). Specifically using a feature selection threshold $P < 0.01$, MC identified 15 positive and 8 negative features. CSF, WM- and non-WM hypointensities, left-inferior-lateral ventricle, as well as the bilateral lateral ventricle and choroid plexus, had larger volumes in AUD than HC. Conversely, the middle-posterior, central and middle-anterior partitions of the CC, brain stem, and left-accumbens, as well as bilateral cerebellar cortex, amygdala, hippocampus, ventral DC, and thalamus had larger volumes in HC than in AUD and achieved an MC-accuracy of 78%. To demonstrate the robustness within-subjects of the classifier, the MC model and features obtained at week 1 were used to predict group membership at week 3, using a feature selection threshold $P < 0.01$. With these constraints MC reached a balanced accuracy of 82% in the classification of AUD and HC at week 3.

Discussion

This study reports significant changes of subcortical volumes in AUD patients, including 31 ± 6% larger ventricles and CSF volume and 11 ± 2% smaller volumes of amygdala, hippocampus, caudate, accumbens, putamen, thalamus, ventral DC, cerebellum, brain stem, and CC studied during the first week of alcohol detoxification. Using these features, MC achieved 80% accuracy in the classification of AUD and HC in the Discovery Cohort and 72% accuracy in the Validation Cohort, consistent with the generalizability of MC to independent samples (H3). This classification accuracy is comparable to that on Discovery Cohorts with SVM, random forest, or other multimodal classifiers combining whole-brain morphometrics (Mackey et al. 2019; Guggenmos et al. 2020) with neuropsychological scores and demographics (Squeglia et al. 2017), based on connectomics (Zhu et al. 2018), electrophysiology (Mumtaz et al. 2018) or epigenetics (Rosato et al. 2019), or combining multimodal biomarkers (Kamarajan et al. 2020) and family history (Kinreich et al. 2019). The higher classification accuracy, sensitivity, and specificity for subcortical volumes, than for other morphometrics (cortical volumes, surface areas, cortical thickness, curvature, and/or folding index), is consistent with hypothesis H1 ("subcortical volumes MC would achieve higher classification accuracy than

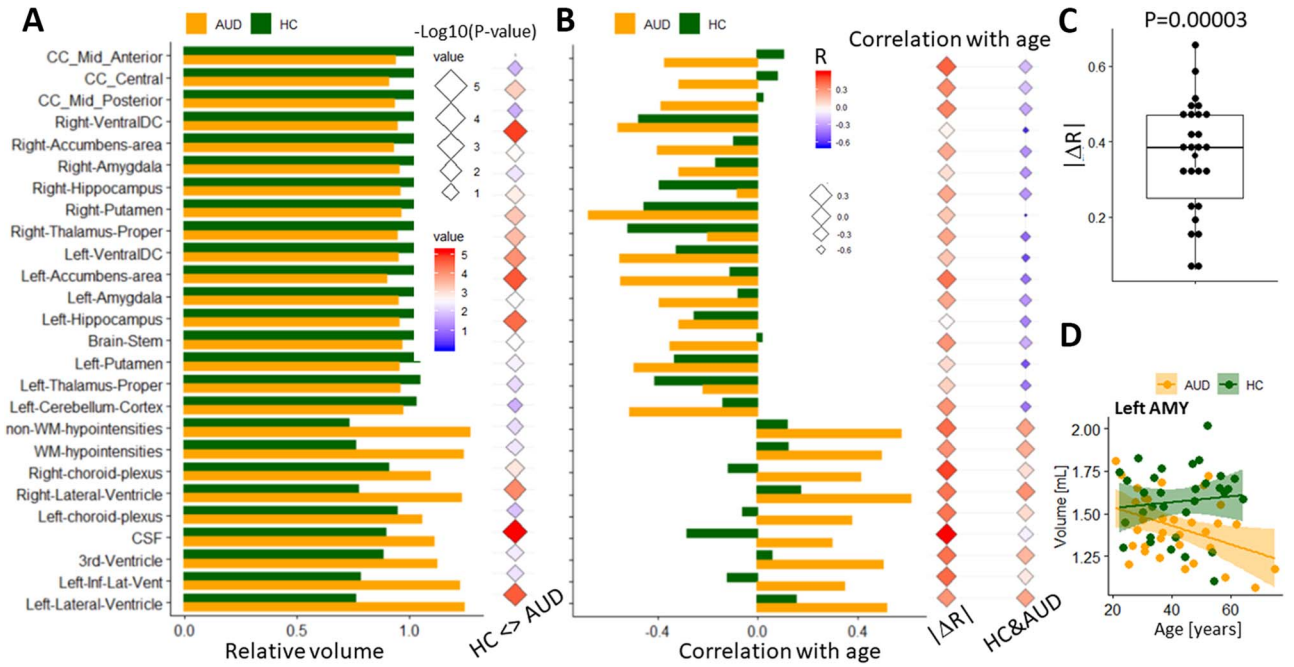

Figure 3. Relative volumes and effect of age. (*A*) Barplot showing the relative volumes of 26 MC-features for AUD patients and HCs and the corresponding statistical group differences (colored diamonds). (*B*) Barplot showing the correlations of the volumes with age (R) and corresponding statistics for the absolute difference in correlation between the groups (|ΔR|) and the average correlation with age across all subjects (HC&AUD) (colored diamonds). (*C*) Boxplot the distribution of absolute differences in correlation with age across MC-features and its statistical significance (P; t-test, two-tailed). (*D*) The volume of the amygdala (AMY) showed a significant negative correlation with age in 33 AUD but not in 32 HC. CSF: cerebrospinal fluid; CC: corpus callosum; Ventral DC: ventral diencephalon. Discovery cohort.

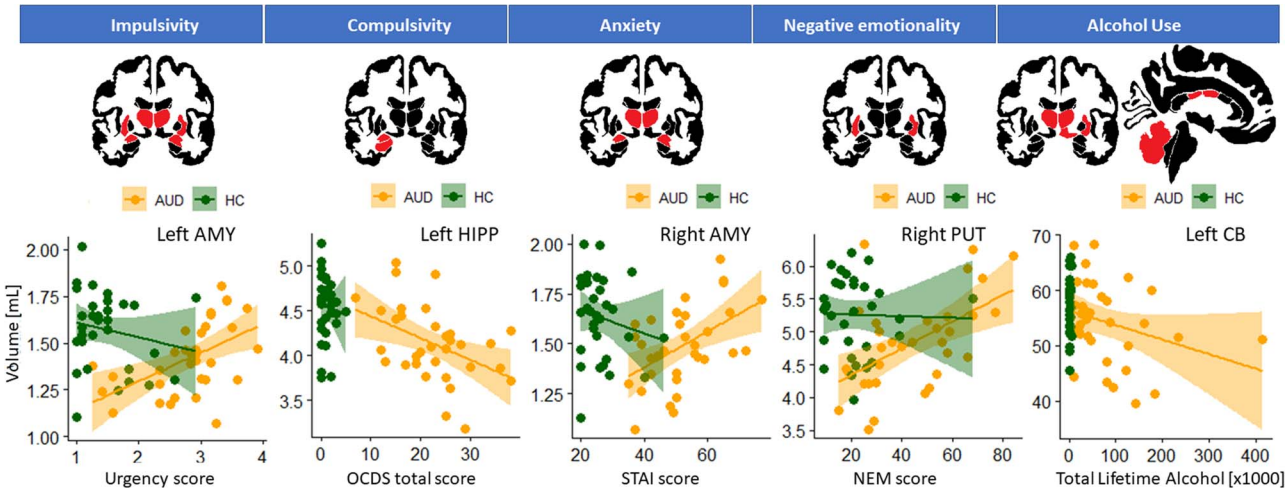

Figure 4. Associations between MC-features and behavior. For illustrative purposes, coronal (left) and sagittal (right) views of a human brain atlas show features that demonstrated linear associations with negative emotions including negative urgency, compulsive drinking (OCDS_total score), anxiety (STAI score), and NEM, as well as TLA use in AUD patients and HCs. AMY: amygdala; HIPP: hippocampus; PUT: putamen; CB: cerebellum. Significance threshold $P = 0.05$, uncorrected (see Table 2). Discovery cohort.

with cortical morphometrics, that its performance would be similar to that of SVM"). MC-features are consistent with prior findings of ventricular enlargement (Pfefferbaum et al. 2001), and GM atrophy in amygdala, hippocampus, cerebellum, basal ganglia, and CC in AUD (Riley et al. 1995; Sowell et al. 1996; Wrase et al. 2008; Shim et al. 2019; Chye et al. 2020). These findings are also consistent with our hypothesis H2 ("the amygdala would emerge as a prominent MC-feature"), and suggest that subcortical volumes are core brain structures negatively affected in AUD.

Several MC-features demonstrated significant effects of age. Particularly the volumes of the third and lateral ventricles, choroid plexus, CSF, as well as WM and non-WM hypointensities, showed increased volume with age, whereas the volumes of

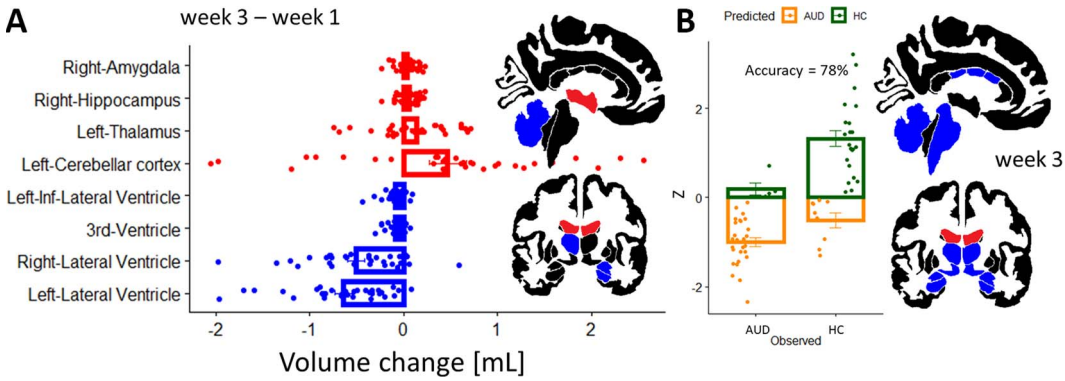

Figure 5. Effect of alcohol detoxification on brain volumes. (A) Barplot and two orthogonal views of the brain template showing MC-features with statistically significant differences in volume between baseline (week 1) and end of detoxification (week 3). (B) Bar plot showing the MC-accuracy in the classification of 32 AUD patients imaged at end of detoxification and the brain atlas showing the features of this classifier. The lateral ventricles (red) consistently showed larger volumes for AUD than for HC; the amygdala, hippocampus, accumbens, ventral DC, thalamus, cerebellum, brain stem and medial regions of the corpus callosum (blue) showed larger volumes for HC than for AUD. Z: positive–negative difference score (see text). Discovery cohort.

the cerebellar cortex, accumbens, putamen, and ventral DC decreased with age across all participants. These findings are consistent with the enlargement of CSF partitions (Rubenstein 1998; Pfefferbaum et al. 2001; Walhovd et al. 2005) and increases in WM hypointenstities (Wei et al. 2019), and the atrophy of the cerebellar cortex, basal ganglia and brain stem that have been reported with age (Raz et al. 2005; Walhovd et al. 2005). Furthermore, the left-amygdala demonstrated significant age-related decreases in AUD but not in HC, supporting hypothesis H4 ("subcortical regions identified by MC, including the amygdala, would show accelerated aging in AUD"). Except for the thalamus and right-hippocampus, all MC-features showed stronger age-correlations in AUD than in HC, and the absolute group differences in the correlations with age were significant across MC-features. These findings are therefore consistent with the hypothesis that alcohol exacerbates the effects of aging in the brain (Sullivan and Pfefferbaum 2019) and expand it to subcortical volumes. Multiple mechanisms have been proposed to contribute to the accelerated aging of the brain with chronic exposure to high doses of alcohol including excitotoxicity, toxic intermediates from alcohol metabolism, disruption of brain energetics and mitochondrial function, dietary factors such as thiamine depletion, and changes in neurotrophic factors among others (Jaatinen and Rintala 2008). Specifically, repeated high-dose alcohol intoxication and withdrawal results in increased excitatory signaling through N-Methyl-D-aspartic acid or N-Methyl-D-aspartate (NMDA) receptors and a concomitant reduction in gamma-aminobutyric acid (GABA) inhibitory neurotransmission that promotes intraneuronal Ca accumulation (Lovinger 1993). Toxic metabolites from alcohol such as acetaldehyde (Rintala et al. 2000) and reactive oxygen species (ROS) generated though cytochrome P450 2E1(CYP2E1) negatively impact neuronal and glial cells (Montoliu et al. 1995; Eysseric et al. 2000). The direct effects of alcohol on brain energy metabolism and its effects on mitochondrial function (Marin-Garcia et al. 1995; Volkow et al. 2013) as well as modification in neurotrophic factors and deficits in key nutrients such as thiamine are also implicated in the accelerated aging of the brain (Jaatinen and Rintala 2008). Additionally heavy chronic alcohol use has been associated with increased deoxyribonucleic acid (DNA) methylation changes associated with aging (Luo et al. 2020).

We report for the first time an association between amygdala volume and negative affect that differed for AUD patients and HCs. Specifically, higher amygdala volume, bilaterally, was associated with higher negative urgency and anxiety in AUD but not in HC, which is consistent with the involvement of the amygdala in the withdrawal/negative emotion stage in AUD.

The volumes of right-amygdala, right-hippocampus and left cerebellum, and thalamus, the third and left-inferior-lateral ventricle, and both lateral ventricles recovered significantly with abstinence (0.9–24.7%), supporting hypothesis H5 ("the volume of the amygdala would recover during detoxification"). These findings are in agreement with prior studies showing a reduction of ventricular enlargement with alcohol abstinence (Schroth et al. 1988; Zipursky et al. 1989; Shear et al. 1994; Sullivan et al. 2000; Pfefferbaum et al. 2001; Zahr et al. 2016). Our findings of recovery of hippocampal, thalamic and amygdala volumes are also consistent with prior reports (Liu et al. 2000; Wrase et al. 2008; Zou et al. 2018). Other studies, however, did not find an association between amygdala volume and abstinence in AUD (Fein et al. 2006). The mechanisms accounting for recovery remain unclear and some have suggested that it reflects WM regeneration (Kipp et al. 2012). In our study, in AUD participants the volume of the amygdala was ~10% smaller than in HCs, and its recovery during detoxification was only partial (<3%), which likely reflect recovery in extracellular water content (De Santis et al. 2020). Furthermore, the recovery of the amygdala volume with detoxification was predicted by baseline measures of amygdala volume, anxiety and negative urgency scores. This evidence of volume recovery with alcohol detoxification could explain prior results of no differences in subcortical volumes between long-term abstinent alcoholics and nonalcoholic controls (Daftary et al. 2019). While at baseline AUD patients had 20–45% larger ventricular and CSF and 5–15% smaller subcortical GM partitions, the recovery of these volumes was only partial (<25% for ventricles and CSF, and <3% for GM nuclei) and did not affect the MC-accuracy, based on subcortical volumes obtained at the end of detoxification (78% accuracy).

For our AUD participants, larger amygdala volumes at baseline were associated with more severe anxiety and impulsivity, consistent with the amygdala's involvement in what is referred to as the "dark side of addiction" (Koob and Volkow 2016). However, since negative emotions, including anxiety (McGue

et al. 1997), as well as smaller amygdalae are associated with a higher risk for AUD (Dager et al. 2015), one would have expected that smaller amygdalae would be associated with more severe negative emotions as previously reported by others in young adults (Daftary et al. 2019; Oshri et al. 2019). The reason for this discrepancy is unclear but it could reflect variability in amygdala volume in AUD. Compared to older AUD patients, younger patients had relatively larger and possibly more reactive amygdalae to stress signals such as CRF, which could make them more vulnerable to atrophy with age. Indeed there is evidence that with aging the amygdala loses some of its reactivity to these stress signals (Kovács et al. 2019). There is also evidence from fMRI studies that the CRF1 receptor antagonist verucerfont, attenuated the amygdala's responses to negative affective stimuli in anxious women with AUD (Schwandt et al. 2016).

The small sample size is the main limitation of our study. Thus, our findings on age-related effects in subcortical regions must be reproduced by future studies. The sample size also limited our ability to properly assess gender differences in brain morphology in AUD and their interaction with age (Sawyer et al. 2017). The HC group lacked test–retest (week1-week3) structural data, which prevented us from studying group-by-week interaction effects on subcortical volumes. The use of both high- and low-resolution scans complicated the analysis and interpretation of results. However, the use of morphometrics from different scan resolutions, which were highly correlated and demonstrated similar MC-features and classification accuracy at baseline and at the end of detoxification, showed the generalization of the results to standard imaging techniques. Although not significant, the difference in classification accuracy between the Validation and Discovery cohorts, both for MC and SVM, may also reflect differences in sample size and clinical variables between participants in the Validation and Discovery cohorts. Nevertheless, the degree of reproducibility of MC is similar to that reported with ML classifiers in AUD (Mackey et al. 2019). Education, number of smokers, and psychiatric symptoms were significantly different between AUD and HC, both in the Discovery and Validation cohorts. Therefore, other variables such as tobacco use could have been responsible for some of the observed effects (Gosnell et al. 2020). TLA ingestion, which correlated with age so that it was largest for older individuals, was also correlated with cerebellar (see Fig. 4), putamen, accumbens, and thalamic volumes though not with the amygdala volume. While these results are consistent with increased age-related GM decline (Sullivan et al. 2018), studies in larger samples are needed to document age × TLA interaction effects on these subcortical GM regions.

The reasons why MC outperformed SVM in the present study are uncertain. SVM tends to be effective in small samples, but it may not perform well when the number of dimensions is comparable to the number of samples due to overfitting in model selection (Cawley and Talbot 2010). Conversely, MC is robust to overfitting because its model selection with only one adjustable parameter is extremely simple. The low sample size in the present study ($N = 65$) and the number of dimensions (45 alcohol-sensitive subcortical regions; mostly CSF partitions and GM nuclei) may have resulted in significant overfitting in the SVM-model selection.

In summary, our findings document significant volumetric changes in subcortical regions including the amygdala that showed exacerbated atrophy with aging but some level of recovery with detoxification in AUD patients. We also document an association between amygdala volume with anxiety and negative urgency that corroborates in humans the involvement of the amygdala in the withdrawal/negative stage, described as the dark side of addiction, in AUD.

Supplementary Material

Supplementary material can be found at *Cerebral Cortex* online.

Notes

We thank Karen Torres, Minoo McFarland, Lori Talagla, David George, Yvonne Horneffer, and Kimberly Herman for their contributions and support. *Conflict of Interest*: None declared.

Funding

National Institute on Alcohol Abuse and Alcoholism (Y1AA-3009).

References

American Psychiatric Association. 2000. *Diagnostic and statistical manual of mental disorders: DSM-IV-TR*. Washington, DC: American Psychiatric Association (APA).

American Psychiatric Association. 2013. *Diagnostic and statistical manual of mental disorders*. Washington DC: American Psychiatric Association (APA).

Anton R, Moak D, Latham P. 1996. The obsessive compulsive drinking scale: a new method of assessing outcome in alcoholism treatment studies. *Arch Gen Psychiatry*. 53:225–231.

Bartlett M. 1937. Properties of sufficiency and statistical tests. *Proc R Soc Lond A*. 160:268–282.

Beck A, Steer R, Garbin M. 1988. Psychometric properties of the Beck depression inventory: twenty-five years of evaluation. *Clin Psychol Rev*. 8:77–100.

Brodersen K, Ong C, Stephan K, Buhmann J. 2010. The balanced accuracy and its posterior distribution. In 20th International Conference on Pattern Recognition. Istanbul, Turkey. 3121–3124.

Cawley G, Talbot N. 2010. On over-fitting in model selection and subsequent selection bias in performance evaluation. *J Mach Learn Res*. 11:2079–2107.

Chye Y, Mackey S, Gutman B, Ching C, Batalla A, Blaine S, Brooks S, Caparelli E, Cousijn J, Dagher A *et al.* 2020. Subcortical surface morphometry in substance dependence: an ENIGMA addiction working group study. *Addict Biol*. 25:e12830.

Conover W, Johnson M, Johnson M. 1981. A comparative study of tests for homogeneity of variances, with applications to the outer continental shelf bidding data. *Technometrics*. 23:351–361.

Cyders M, Smith G, Spillane N, Fischer S, Annus A, Peterson C. 2007. Integration of impulsivity and positive mood to predict risky behavior: development and validation of a measure of positive urgency. *Psychol Assess*. 19:107:118.

Daftary S, Enkevort E, Kulikova A, Legacy M, Brown E. 2019. Relationship between depressive symptom severity and amygdala volume in a large community-based sample. *Psychiatry Res Neuroimaging*. 283:77–82.

Dager A, McKay D, Kent JJ, Curran J, Knowles E, Sprooten E, Göring H, Dyer T, Pearlson G, Olvera R *et al.* 2015. Shared genetic factors influence amygdala volumes and risk for alcoholism. *Neuropsychopharmacology*. 40:412–420.

De Santis S, Cosa-Linan A, Garcia-Hernandez R, Dmytrenko L, Vargova L, Vorisek I, Stopponi S, Bach P, Kirsch P, Kiefer F *et al*. 2020. Chronic alcohol consumption alters extracellular space geometry and transmitter diffusion in the brain. *Sci Adv*. 6:eaba0154.

Eysseric H, Gonthier B, Soubeyran A, Richard M, Daveloose D, Barret L. 2000. Effects of chronic ethanol exposure on acetaldehyde and free radical production by astrocytes in culture. *Alcohol*. 21:117–125.

Fein G, Landman B, Tran H, McGillivray S, Finn P, Barakos J, Moon K. 2006. Brain atrophy in long-term abstinent alcoholics who demonstrate impairment on a simulated gambling task. *Neuroimage*. 32:1465–1471.

Fischl B, Salat D, Busa E, Albert M, Dieterich M, Haselgrove C, van der Kouwe A, Killiany R, Kennedy D, Klaveness S *et al*. 2002. Whole brain segmentation: automated labeling of neuroanatomical structures in the human brain. *Neuron*. 33:341–355.

Glasser M, Sotiropoulos S, Wilson J, Coalson T, Fischl B, Andersson J, Xu J, Jbabdi S, Webster M, Polimeni J *et al*. 2013. The minimal preprocessing pipelines for the human connectome project. *Neuroimage*. 80:105–124.

Gosnell S, Meyer M, Jennings C, Ramirez D, Schmidt J, Oldham J, Salas R. 2020. Hippocampal volume in psychiatric diagnoses: should psychiatry biomarker research account for comorbidities? *Chronic Stress*. 4:2470547020906799.

Guggenmos M, Schmack K, Sekutowicz M, Garbusow M, Sebold M, Sommer C, Smolka M, Wittchen H, Zimmermann U, Heinz A *et al*. 2017. Quantitative neurobiological evidence for accelerated brain aging in alcohol dependence. *Transl Psychiatry*. 7:1279.

Guggenmos M, Schmack K, Veer I, Lett T, Sekutowicz M, Sebold M, Garbusow M, Sommer C, Wittchen H, Zimmermann U *et al*. 2020. A multimodal neuroimaging classifier for alcohol dependence. *Sci Rep*. 10:298.

Jaatinen P, Rintala J. 2008. Mechanisms of ethanol-induced degeneration in the developing, mature, and aging cerebellum. *Cerebellum*.

Kamarajan C, Ardekani B, Pandey A, Kinreich S, Pandey G, Chorlian D, Meyers J, Zhang J, Bermudez E, Stimus A *et al*. 2020. Random Forest classification of alcohol use disorder using fMRI functional connectivity, neuropsychological functioning, and impulsivity measures. *Brain Sci*. 10:115.

Kinreich S, Meyers J, Maron-Katz A, Kamarajan C, Pandey A, Chorlian D, Zhang J, Pandey G, Subbie-Saenz de Viteri S, Pitti D *et al*. 2019. Predicting risk for alcohol use disorder using longitudinal data with multimodal biomarkers and family history: a machine learning study. *Mol Psychiatry*. doi: 10.1038/s41380-41019-40534-x (published online ahead of print).

Kipp M, Victor M, Martino G, Franklin R. 2012. Endogeneous remyelination: findings in human studies. *CNS Neurol Disord Drug Targets*. 11:598–609.

Koob G, Le Moal M. 2005. Plasticity of reward Neurocircuitry and the 'Dark Side' of drug addiction. *Nat Neurosci*. 8:1442–1444.

Koob G, Volkow N. 2016. Neurobiology of addiction: a neurocircuitry analysis. *Lancet Psychiatry*. 3:760–773.

Kovács L, Berta G, Csernus V, Ujvári B, Füredi N, Gaszner B. 2019. Corticotropin-releasing factor-producing cells in the paraventricular nucleus of the hypothalamus and extended amygdala show age-dependent FOS and FOSB/DeltaFOSB immunoreactivity in acute and chronic stress models in the rat. *Front Aging Neurosci*. 11:274.

Liu R, Lemieux L, Shorvon S, Sisodiya S, Duncan J. 2000. Association between brain size and abstinence from alcohol. *Lancet*. 355:1969–1970.

Lovinger D. 1993. Excitotoxicity and alcohol-related brain damage. *Alcohol Clin Exp Res*. 17:19–27.

Luo A, Jung J, Longley M, Rosoff D, Charlet K, Muench C, Lee J, Hodgkinson C, Goldman D, Horvath S *et al*. 2020. Epigenetic aging is accelerated in alcohol use disorder and regulated by genetic variation in APOL2. *Neuropsychopharmacology*. 45:327–336.

Mackey S, Allgaier N, Chaarani B, Spechler P, Orr C, Bunn J, Allen N, Alia-Klein N, Batalla A, Blaine S *et al*. 2019. Mega-analysis of gray matter volume in substance dependence: general and substance-specific regional effects. *Am J Psychiatry*. 176:119–128.

Marin-Garcia J, Ananthakrishnan R, Goldenthal M. 1995. Heart mitochondria response to alcohol is different than brain and liver. *Alcohol Clin Exp Res*. 19:1463–1466.

McGue M, Slutske W, Taylor J, Lacono W. 1997. Personality and substance use disorders: I. effects of gender and alcoholism subtype. *Alcohol Clin Exp Res*. 21:513–520.

Montoliu C, Sancho-Tello M, Azorin I, Burgal M, Vallés S, Renau-Piqueras J, Guerri C. 1995. Ethanol increases cytochrome P4502E1 and induces oxidative stress in astrocytes. *J Neurochem*. 65:2561–2570.

Mumtaz W, Saad M, Kamel N, Ali S, Malik A. 2018. An EEG-based functional connectivity measure for automatic detection of alcohol use disorder. *Artif Intell Med*. 84:79–89.

Oshri A, Gray J, Owens M, Liu S, Duprey E, Sweet L, MacKillop J. 2019. Adverse childhood experiences and Amygdalar reduction: high-resolution segmentation reveals associations with subnuclei and psychiatric outcomes. *Child Maltreat*. 24:400–410.

Pfefferbaum A, Rosenbloom M, Deshmukh A, Sullivan E. 2001. Sex differences in the effects of alcohol on brain structure. *Am J Psychiatry*. 158.

Pfefferbaum A, Sullivan E, Rosenbloom M, Mathalon D, Lim K. 1998. A controlled study of cortical gray matter and ventricular changes in alcoholic men over a 5-year interval. *Arch Gen Psychiatry*. 55:805–912.

Ramirez V, Wiers C, Wang G, Volkow N. 2020. Personality traits in substance use disorders and obesity when compared to healthy controls. *Addiction*. doi: 10.1111/add.15062 (published online ahead of print).

Raz N, Lindenberger U, Rodrigue K, Kennedy K, Head D, Williamson A, Dahle C, Gerstorf D, Acker J. 2005. Regional brain changes in aging healthy adults: general trends, individual differences and modifiers. *Cereb Cortex*. 15:1676–1689.

Riley E, Mattson S, Sowell E, Jernigan T, Sobel D, Jones K. 1995. Abnormalities of the corpus callosum in children prenatally exposed to alcohol. *Alcohol Clin Exp Res*. 19:1198–1202.

Rintala J, Jaatinen P, Parkkila S, Sarviharju M, Kiianmaa K, Hervonen A, Niemelä O. 2000. Evidence of acetaldehyde-protein adduct formation in rat brain after lifelong consumption of ethanol. *Alcohol Alcohol*. 35:458–463.

Rosato A, Chen X, Tanaka Y, Farrer L, Kranzler H, Nunez Y, Henderson D, Gelernter J, Zhang H. 2019. Salivary microRNAs identified by small RNA sequencing and machine learning as potential biomarkers of alcohol dependence. *Epigenomics*. 11:739–749.

Rubenstein E. 1998. Relationship of senescence of cerebrospinal fluid circulatory system to dementias of the aged. *Lancet*. 351:283–285.

Saunders J, Aasland O, Babor T, de la Fuente J, Grant M. 1993. Development of the alcohol use disorders identification test (AUDIT): WHO collaborative project on early detection of persons with harmful alcohol consumption-II. *Addiction*. 88:791–804.

Sawyer K, Oscar-Berman M, Barthelemy O, Papadimitriou G, Harris G, Makris N. 2017. Gender dimorphism of brain reward system volumes in alcoholism. *Psychiatry Res Neuroimaging*. 2017:15–25.

Schroth G, Naegele T, Klose U, Mann K, Petersen D. 1988. Reversible brain shrinkage in abstinent alcoholics, measured by MRI. *Neuroradiology*. 30:385–389.

Schwandt M, Cortes C, Kwako L, George D, Momenan R, Sinha R, Grigoriadis D, Pich E, Leggio L, Heilig M. 2016. The CRF1 antagonist verucerfont in anxious alcohol-dependent women: translation of neuroendocrine, but not of anti-craving effects. *Neuropsychopharmacology*. 41:2818–2829.

Shapiro S, Wilk M. 1965. An analysis of variance test for normality (complete samples). *Biometrika*. 52:591–611.

Shear P, Jernigan T, Butters N. 1994. Volumetric magnetic resonance imaging quantification of longitudinal brain changes in abstinent alcoholics. *Alcohol Clin Exp Res*. 18: 172–176.

Shen X, Finn E, Scheinost D, Rosenberg M, Chun M, Papademetris X, Constable R. 2017. Using connectome-based predictive modeling to predict individual behavior from brain connectivity. *Nat Protoc*. 12:506–518.

Shim J, Kim Y, Kim S, Baek H. 2019. Volumetric reductions of subcortical structures and their localizations in alcohol-dependent patients. *Front Neurol*. 10:247.

Skinner H, Allen B. 1982. Alcohol dependence syndrome: measurement and validation. *J Abnorm Psychol*. 91:199–209.

Skinner H, Sheu W. 1982. Reliability of alcohol use indices. The lifetime drinking history and the MAST. *J Stud Alcohol*. 43:1157–1170.

Sobell L, Sobell M. 1996. Alcohol abuse and smoking: dual recoveries. *Alcohol Health Res World*. 20:124–127.

Sowell E, Jernigan T, Mattson S, Riley E, Sobel D, Jones K. 1996. Abnormal development of the cerebellar vermis in children prenatally exposed to alcohol: size reduction in lobules I–V. *Alcohol Clin Exp Res*. 20:31–34.

Spielberger CD, Gorsuch RL, Lushene R, Vagg PR, Jacobs GA. 1983. *Manual for the State–Trait Anxiety Inventory*. Palo Alto, CA: Consulting Psychologists Press.

Squeglia L, Ball T, Jacobus J, Brumback T, McKenna B, Nguyen-Louie T, Sorg S, Paulus M, Tapert S. 2017. Neural predictors of initiating alcohol use during adolescence. *Am J Psychiatry*. 174:172–185.

Sullivan E, Pfefferbaum A. 2019. Brain–behavior relations and effects of aging and common comorbidities in alcohol use disorder: a review. *Neuropsychology*. 33:760–780.

Sullivan E, Rosenbloom M, Lim K, Pfefferbaum A. 2000. Longitudinal changes in cognition, gait, and balance in abstinent and relapsed alcoholic men: relationships to changes in brain structure. *Neuropsychology*. 14:178–188.

Sullivan E, Zahr N, Sassoon S, Thompson W, Kwon D, Pohl K, Pfefferbaum A. 2018. The role of aging, drug dependence, and hepatitis C comorbidity in alcoholism cortical compromise. *JAMA Psychiatry*. 75:474–483.

Sullivan JT, Sykora K, Schneiderman J, Naranjo CA, Sellers EM. 1989. Assessment of alcohol withdrawal: the revised clinical institute withdrawal assessment for alcohol scale (CIWA-Ar). *Br J Addict*. 84:1353–1357.

Tellegen A, Waller N. 2008. Exploring personality through test construction: Development of the Multidimensional Personality Questionnaire. In: *The SAGE Handbook of Personality Theory and Assessment*. London, England.

Thayer R, Hagerty S, Sabbineni A, Claus E, Hutchison K, Weiland B. 2016. Negative and interactive effects of sex, aging, and alcohol abuse on gray matter morphometry. *Hum Brain Mapp*. 2016:6.

Tomasi D, Volkow N. 2020. Network connectivity predicts language processing in healthy adults. *Hum Brain Mapp*. 41.

Tomasi D, Wiers C, Shokri-Kojori E, Zehra A, Ramirez V, Freeman C, Burns J, Kure Liu C, Manza P, Kim S *et al*. 2019. Association between reduced brain glucose metabolism and cortical thickness in alcoholics: evidence of neurotoxicity. *Int J Neuropsychopharmacol*. 22:548–559.

Volkow N, Kim S, Wang G, Alexoff D, Logan J, Muench L, Shea C, Telang F, Fowler J, Wong C *et al*. 2013. Acute alcohol intoxication decreases glucose metabolism but increases acetate uptake in the human brain. *Neuroimage*. 64:277–283.

Walhovd K, Fjell A, Reinvang I, Lundervold A, Dale A, Eilertsen D, Quinn B, Salat D, Makris N, Fischl B. 2005. Effects of age on volumes of cortex, white matter and subcortical structures. *Neurobiol Aging*. 26:1261–1270.

Wechsler D. 1999. *Wechsler Abbreviated Scale of Intelligence Manual*.

Wei K, Tran T, Chu K, Borzage M, Braskie M, Harrington M, King K. 2019. White matter hypointensities and hyperintensities have equivalent correlations with age and CSF beta-amyloid in the nondemented elderly. *Brain Behav*. 9:e01457.

Wrase J, Makris N, Braus D, Mann K, Smolka M, Kennedy D, Caviness V, Hodge S, Tang L, Albaugh M *et al*. 2008. Amygdala volume associated with alcohol abuse relapse and craving. *Am J Psychiatry*. 165:1179–1184.

Young S, Bowman A. 1995. Nonparametric analysis of covariance. *Biometrics*. 51:920–931.

Zahr N, Pohl K, Saranathan M, Sullivan E, Pfefferbaum A. 2019. Hippocampal subfield CA2+3 exhibits accelerated aging in alcohol use disorder: a preliminary study. *Neuroimage Clin*. 22:101764.

Zahr N, Rohlfing T, Mayer D, Luong R, Sullivan E, Pfefferbaum A. 2016. Transient CNS responses to repeated binge ethanol treatment. *Addict Biol*. 21:1199–1216.

Zhao Q, Pfefferbaum A, Podhajsky S, Pohl K, Sullivan E. 2020. Accelerated aging and motor control deficits are related to regional deformation of central cerebellar white matter in alcohol use disorder. *Addict Biol*. 25:e12746.

Zhu X, Du X, Kerich M, Lohoff F, Momenan R. 2018. Random forest based classification of alcohol dependence patients and healthy controls using resting state MRI. *Neurosci Lett*. 676:27–33.

Zipursky R, Lim K, Pfefferbaum A. 1989. MRI study of brain changes with short-term abstinence from alcohol. *Alcohol Clin Exp Res*. 13:664–666.

Zou X, Durazzo T, Meyerhoff D. 2018. Regional brain volume changes in alcohol-dependent individuals during short-term and long-term abstinence. *Alcohol Clin Exp Res*. 42:1062–1072.